

# Dynamic wetting properties of PDMS pseudo-brushes:

## Four-Phase contact point dynamics case

Peyman Rostami,<sup>1</sup> Mohammad Ali Hormozi,<sup>2</sup> Olaf Soltwedel,<sup>2</sup> Reza Azizmalayeri,<sup>1</sup> Regine von Klitzing,<sup>2</sup> and Günter.K Auernhammer<sup>1</sup>

<sup>1</sup>*Abteilung Polymergrenzflächen, Leibniz-Institut für Polymerforschung Dresden e.V, Dresden, 01069, Germany*

<sup>2</sup>*Soft Matter at Interfaces, Department of Physics, Technical University of Darmstadt, Darmstadt, 64289, Germany*

(\*Electronic mail: auernhammer@ipfdd.de)

(\*Electronic mail: klitzing@smi.tu-darmstadt.de)

(\*Electronic mail: rostami@ipfdd.de)

(Dated: 9th March 2023)

### I. DESCRIPTION OF XRR METHOD:

To determine the brush thickness, we employed XRR (x-ray reflectivity) using a Bruker D8 Advanced, equipped with a CuK $\alpha$  anode ( $\lambda = 1.54 \text{ \AA}$ ). In analogy to classical optics the reflectivity from x-rays is mainly given by the interference between the photons reflected from changes of the index of refraction along the surface normal ( $z$ -direction) across a surface layer. With its small wavelength, the index of refraction ( $n$ ) depends linearly on the electron density ( $\rho_{el}$ ), with  $n = 1 - \delta$  and  $\delta = \frac{\lambda^2}{2\pi} r_e \rho_{el}$ , of the constituting polymer brushes and the substrate. Together with the classical electron radius ( $r_e$ ) the electron density can be expressed as scattering length density  $SLD = r_e \rho_{el}$  which we use here. Since the index of refraction deviates little from unity, the measured reflectivity  $R$  can be approximated by the *Fresnel*-reflectivity ( $R_{Fres}$ ) of an infinitely sharp interface modulated by interference effects from the surface layer.<sup>1</sup> Above three critical angles of total external reflection, where multiple scattering can be neglected, the reflectivity is given by the kinematic approximation, which is basically the squared *Fourier*-transform of the *SLD*-gradient in the  $z$ -direction.<sup>2</sup>

$$\frac{R}{R_{Fres}} = \left| \frac{1}{SLD_{Si}} \int \frac{d}{dz} (SLD(z)) \cdot e^{-iQ_z z} dz \right|^2 \quad (1)$$

Here,  $SLD_{Si}$  is the silicon substrates *SLD*, and  $Q_z$  is the wave vector transfer normal to the surface ( $Q_z = \frac{4\pi}{\lambda} \sin(\alpha_i)$  with  $\alpha_i$  being the incidence angle). Also the measured reflectivity is foot print corrected and normalized to the primary beam in order to make them comparable to the simulations.

To gain satisfactory fit results and consistency we use 3 slabs to parameterize the brushes *SLD*-profile. The interfaces between the slabs are smeared out with a *Gauss* error function. With this each slab is described by its *SLD* and thickness and each interface is characterized by a roughness parameter. To overcome over-parametrization the thickness of the substrate-adjacent and the air adjacent slabs are constraint to twice the roughness of the bulk materials respectively ( $l_1 = 2\sigma_1$ ,  $l_3 = 2\sigma_3$ ). Main advantage of the kinematic approximation is the intuitive dependency of the measured reflectivity and *SLD*-profile which helps to guess reasonable initial parametrization. For exact calculations we make use of the *Ables*-matrix

formalism.<sup>3</sup> The calculated reflectivity is then convoluted with the angular divergence and of the spectrometer (10 mrad) and compared to the measured reflectivity. Then the *Levenberg-Marquardt*-algorithm is used to vary the *SLD*-profile parameters with the aim to minimize the deviation between the measured reflectivity in a recursive way.<sup>4,5</sup> Additionally we fit a constant background to the simulated reflectivity, to account for the samples diffuse scattering and detector dark current. With this we refine the *SLD*-profile along the  $z$ -direction with sub nm resolution<sup>6</sup>.

### II. AFM MEASUREMENTS

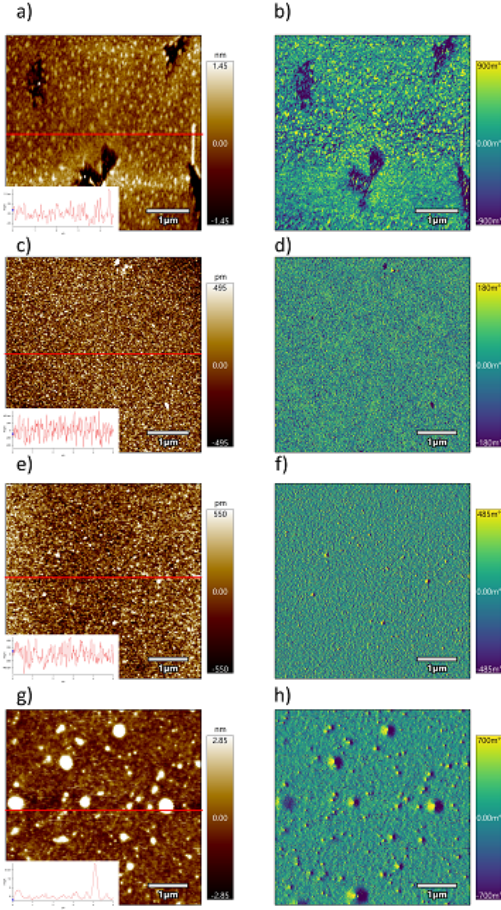
Further AFM experiments on bare glass, DMS-T5, DMS-T21 and DMS-T25 are presented here (FigS. 1).

### III. RELATION BETWEEN THE PDMS PSEUDO BRUSHES TO THE PROPERTY OF USED POLYMER MELT

For PDMS adsorbed layer, it is shown that the thickness should be a function of polymerization index ( $l_2 \sim \sqrt{N}$ )<sup>7</sup>. This relation is exactly what we observed in our data FigS. 2

### IV. EFFECT OF HUMIDITY ON PDMS PSEUDO-BRUSHES

Due to the strong absorption of CuK $\alpha$ - radiation in bulk liquids, we were not able to access the layer thickness applying XRR. Instead, we explored the response of the PDMS pseudo-brush thickness upon varying access water via water vapour. The XRR data show no significant change in the refined *SLD* – profile, as expected for hydrophobic thin films. We attribute the small non-monotonic changes to aging effects rather than the water impact, since the order of the measurement was ambient – 0% r.h. – 100 % r.h.. Additional repetitions revealed no further detectable *SLD*-profile changes. At this point one has to conclude that the PDMS-pseudo-brush is stiff in contact with water and does not tend to swell. Fresnel-normalized

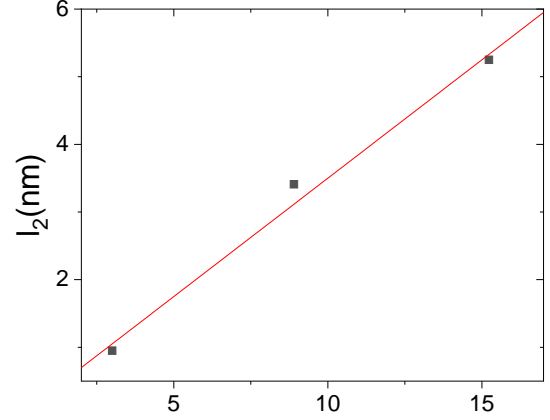


FigS. 1. The height and phase image of the glass substrate a) and b) for bare glass, c) and d) for coated with PDMS pseudo-brushes DMS-T5 ( $770 \frac{\text{g}}{\text{mol}}$ ), e) and f) for DMS-T21 ( $5970 \frac{\text{g}}{\text{mol}}$ ) and g) and h) for DMS-T25 ( $17250 \frac{\text{g}}{\text{mol}}$ ) respectively. The cross section of each sample is shown in the inset of height image.

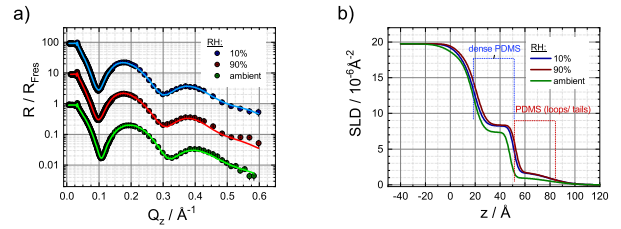
x-ray reflectivities (a) and corresponding refined scattering length density profiles (b) of the DMS-T21 for varying relative humidity. The measured reflectivity are the circles with error bars, which are mostly smaller than the symbol size. The fitted reflectivity (a) and their corresponding scattering length profiles (b) are the solid lines having the same color code. To enhance readability the reflectivity curves are shifted by a factor of 10 against each other. The Si-surface is set to  $z = 0$  (b) and for increasing  $z$  the SLD-profiles first probe the interfacial layer and then bulk gaseous phase.

## V. COMPARING THE VISCOELASTIC DISSIPATION IN THE PDMS PSEUDO-BRUSHES WITH PDMS THICK LAYER

Based on what is presented in the main text, the PDMS pseudo-brushes have less pinning compared to the glass silanized substrates. The open question would be what is the



FigS. 2. Relation between the brush thickness versus polymer index.



FigS. 3. Fresnel-normalized x-ray reflectivities (a) and corresponding refined scattering length density profiles (b). The measured reflectivity are the circles with error bars, which are mostly smaller than the symbol size in different humidities.

effect of viscoelasticity of these brushes on the wetting and how much energy is dissipated in the brushes. To avoid any confusion the energy dissipation on PDMS pseudo-brushes is compared to thick PDMS layers (as described in the previous study<sup>8</sup> (different composition of PDMS, Sylgard 184)). The main idea behind this comparison is that the thick PDMS layers and pseudo-brushes have much less pinning compared to the silanized substrates. This argument will help us to evaluate the energy dissipation cost by introducing the PDMS pseudo-brushes.

The wetting behaviour on soft substrates in static<sup>9,10</sup> and dynamic cases<sup>11-13</sup> are studied for a long time. In static cases, researchers are more interested in the shape and the height of ridge (i.e. microscopic protrusion of the contact line). On the other hand, in dynamic wetting cases, the important point is the energy dissipation in soft substrate due to the movement of ridge along with contact line. In this study, since we are interested on dynamic wetting on brushes, we follow the same analogy as presented by Leibler et. al.<sup>14</sup>. To explain the situation, consider a drop seated on a solid substrate with the shear modulus of  $G$ . The surface tension of liquid-gas interface has a vertical component ( $\gamma \sin(\theta)$ ) which will be balanced with elasticity of substrate ( $\gamma \sin(\theta) \sim Ge$ ). Where  $e$  is the height

of substrate deformation. It should be mentioned that on the substrates, the deformation happens not only at the contact line but forms a cusp underneath of drop. In this study, for simplicity, we estimate that the deformation is balanced at the contact line. On the PDMS pseudo-brushes, the deformation is in order of brush thickness, so by considering the surface tension as ( $\gamma = 72 \frac{mN}{m}$ ), contact angle ( $\theta \sim 90^\circ$ ), the shear modulus is in order of  $\sim MPa$ . On the other two extremes on hard substrates ( $G > 10^9 Pa$ ), the ridge height is in order of angstrom ( $\text{\AA}$ ) and for soft substrates ( $G \sim 200kPa$ ), in order of  $300nm$  (in a good agreement with published works<sup>15,16</sup>.) So the deformation and shear modulus of the PDMS pseudo-brushes are in an intermediate state. In the dynamic case, the relaxation time of the PDMS pseudo-brushes is a crucial parameter<sup>14</sup>. The relaxation time can be calculated from the following equation (Eq. 2)<sup>17</sup>:

$$\tau = \frac{\xi a^2 N^2}{6\pi^2 k_B T} \quad (2)$$

where  $a$  is the polymer monomer size (for PDMS case  $a = 0.46nm$ ),  $N$  is the polymerization index from table (Table III),  $k_B$  and  $T$  are Boltzmann constant and temperature respectively.

The monomeric friction coefficient  $\xi$  can be back calculated from the kinematic viscosity of melts (Eq. 3).

$$\nu = \frac{\xi b^2 N_A N}{36m_0} \quad (3)$$

where  $b$  is the Kuhn length of the polymer (in the present study  $b = 0.2nm$ ),  $N_A$  is Avogadro's number and  $m_0$  is molecular mass of the monomer (for PDMS  $m_0 = 74.1(\frac{g}{mol})$ ).

Substituting Eqs. (3) to (2), the relaxation time for each sample can be calculated. The relaxation time ( $\tau$ ) is  $4.3ns$ ,  $0.75\mu s$  and  $11\mu s$  for DMS-T5, DMS-T21 and DMS-T25 samples. By having the brush height one can calculate the relaxation velocity of brushes which are in order of  $\sim m/s$  to  $\sim mm/s$ , based on contact line velocities ( $\sim mm/s$ ) for high molar mass PDMS pseudo-brushes, the polymer is not fully relaxed.

The Rouse model also suggests that the dissipated power  $P$  is a function of liquid viscosity, contact line velocity, surface tension and shear modulus ( $P \sim \eta_{brush} V^2 (\frac{\gamma}{G^2})$ )<sup>14</sup>. By considering all the parameter identical but the shear modulus, the dissipated power in PDMS pseudo-brushes ( $G \sim MPa$ ) is few percents ( $\sim 2\%$ ) of power dissipation in a soft substrate ( $G \sim 200kPa$ ). In conclusion, by introducing PDMS pseudo-brushes, due to the less pinning, the force needed to

move the drop over the surface is reduced by 90% compared to the one on glass silanized substrate. On the other hand, the dissipated power due to the ridge formation is significantly lower than soft substrates (e.g. thick PDMS layers). Combination of these two facts can explain the higher mobility of drops on the PDMS pseudo-brushes.

## REFERENCES

- <sup>1</sup>K. Kjaer, "Some simple ideas on x-ray reflection and grazing-incidence diffraction from thin surfactant films," *Physica B: Condensed Matter* **198**, 100–109 (1994).
- <sup>2</sup>J. Als-Nielsen and D. McMorrow, *Elements of modern X-ray physics*, 2nd ed. (Wiley-Blackwell, Hoboken, NJ, 2011).
- <sup>3</sup>F. Abelès, "La théorie générale des couches minces," *Journal de Physique et le Radium* **11**, 307–309 (1950).
- <sup>4</sup>K. Levenberg, "A method for the solution of certain non-linear problems in least squares," *Quarterly of Applied Mathematics* **2**, 164–168 (1944).
- <sup>5</sup>D. W. Marquardt, "An algorithm for least-squares estimation of nonlinear parameters," *Journal of the Society for Industrial and Applied Mathematics* **11**, 431–441 (1963).
- <sup>6</sup>D. Kesal, S. Christau, M. Trapp, P. Krause, and R. von Klitzing, "The internal structure of PMETAC brush/gold nanoparticle composites: a neutron and x-ray reflectivity study," *Physical Chemistry Chemical Physics* **19**, 30636–30646 (2017).
- <sup>7</sup>L. Léger, E. Raphaël, and H. Hervet, "Surface-anchored polymer chains: Their role in adhesion and friction," *Polymers in confined environments*, 185–225 (1999).
- <sup>8</sup>L. Chen, G. K. Auernhammer, and E. Bonaccorso, "Short time wetting dynamics on soft surfaces," *Soft Matter* **7**, 9084–9089 (2011).
- <sup>9</sup>R. Pericet-Camara, G. K. Auernhammer, K. Koynov, S. Lorenzoni, R. Raiteri, and E. Bonaccorso, "Solid-supported thin elastomer films deformed by microdrops," *Soft Matter* **5**, 3611–3617 (2009).
- <sup>10</sup>B. Zhao, E. Bonaccorso, G. K. Auernhammer, and L. Chen, "Elasticity-to-capillarity transition in soft substrate deformation," *Nano Letters* **21**, 10361–10367 (2021).
- <sup>11</sup>M. Shanahan, "The spreading dynamics of a liquid drop on a viscoelastic solid," *Journal of Physics D: Applied Physics* **21**, 981 (1988).
- <sup>12</sup>S. Karpitschka, S. Das, M. van Gorcum, H. Perrin, B. Andreotti, and J. H. Snoeijer, "Droplets move over viscoelastic substrates by surfing a ridge," *Nature communications* **6**, 1–7 (2015).
- <sup>13</sup>J. Dervaux, M. Roché, and L. Limat, "Nonlinear theory of wetting on deformable substrates," *Soft Matter* **16**, 5157–5176 (2020).
- <sup>14</sup>D. Long, A. Ajdari, and L. Leibler, "How do grafted polymer layers alter the dynamics of wetting?" *Langmuir* **12**, 1675–1680 (1996).
- <sup>15</sup>S. J. Park, B. M. Weon, J. S. Lee, J. Lee, J. Kim, and J. H. Je, "Visualization of asymmetric wetting ridges on soft solids with x-ray microscopy," *Nature communications* **5**, 1–7 (2014).
- <sup>16</sup>R. Pericet-Cámara, A. Best, H.-J. Butt, and E. Bonaccorso, "Effect of capillary pressure and surface tension on the deformation of elastic surfaces by sessile liquid microdrops: an experimental investigation," *Langmuir* **24**, 10565–10568 (2008).
- <sup>17</sup>S. Edwards and M. Doi, "The theory of polymer dynamics," (1986).